Effect of Microstructure and Temperature on Hydrogen Diffusion and Trapping in X70 grade Pipeline Steel and its Weldments

Magnus Skjellerudsveen *NTNU*[1]*, 7491 Trondheim, Norway, skjeller@alumni.ntnu.no*
Odd M. Akselsen *NTNU/SINTEF*[2]*, 7034 Trondheim, Norway, odd.m.akselsen@sintef.no*
Vigdis Olden *SINTEF, 7034 Trondheim, Norway, vigdis.olden@sintef.no*
Roy Johnsen *NTNU, 7491 Trondheim, Norway, roy.johnsen@ntnu.no*
Anna Smirnova *NTNU, 7491 Trondheim, Norway, anna.smirnova@ntnu.no*

Summary

Hydrogen diffusion was studied in API grade X70 pipeline steel, simulated coarse grained heat affected zone (HAZ) and weld metal of type HBQ Coreweld using the electrochemical permeation technique. Hydrogen diffusion measurements were carried out at 25°C, 50°C and 70°C. The results were similar for all three metals with the average values of effective diffusion coefficient at 25°C ranging from 1.26×10^{-7} to 1.22×10^{-6}cm^2/s. The values decreased in the order: HBQ Coreweld metal > X70 grade steel > simulated HAZ. The metals showed similar response to increased temperature with respect to the diffusion coefficient. The simulated HAZ showed the highest values for the sub-surface hydrogen concentration, and the value did not vary significantly as a function of temperature for any of the materials. The number of reversible trapping sites was in the order of 10^{19} sites/cm^3. The values of their binding energy varied from 34 to 41 kJ/mol.

1 Introduction

The detrimental effects of hydrogen in steel are well established [1, 2, 3, 4, 5, 6, 7] and one of the main issues when it comes to structural integrity of offshore installations. Several theories as to why hydrogen embrittlement occurs have been postulated with the Hydrogen Enhanced Local Plasticity (HELP) [1, 2, 8, 9] and Hydrogen Enhanced Decohesion (HEDE) [3, 9, 10] theories being increasingly accepted. Common for these two theories is that crack initiation and propagation are dependent on the supply of hydrogen to a critical region through diffusion. Hydrogen cracking is observed to be a stepwise process where abrupt crack growth occurs between periods of no macroscopic change [11, 12].

The heat affected zone (HAZ) adjacent to the weld zone is traditionally the critical area for hydrogen embrittlement, but increasing quality of the base metal has led to the problem shifting to the actual weld metal [13]. The hydrogen diffusion of both weld metal, heat affected base metal and the untreated base metal is therefore of interest. Investigations of hydrogen diffusion have been carried out on similar alloys [14, 15], but with so many parameters for welding, steel production etc., it is difficult to confirm the transferability of results from one system to another. The aim of this work is to determine the diffusion coefficient of hydrogen, effective sub-surface

[1]Norwegian University of Science and Technology
[2]SINTEF Materials and Chemistry

hydrogen concentration and corresponding trapping parameters in an X70 grade pipeline steel and its weldments.

2 Basis for Calculations

The lattice diffusion coefficient for hydrogen in steel is given by:

$$D_l = D_0 exp\left(\frac{-E_l}{RT}\right), \tag{1}$$

where E_l =5.69 kJ/mol is the energy barrier for hydrogen jumps between two lattice points and D_0 is 7.23×10^{-4} cm^2/s [16]. The values are valid in the temperature range between -40°C and 80°C.

The effective diffusion coefficient in a material, D_{eff}, differs from D_l because of traps and can be estimated for a sample according to ISO 17081:2004 [17] as:

$$D_{eff} = \frac{L^2}{6t_{lag}}, \tag{2}$$

where L is the specimen thickness and t_{lag} is the time taken for the permeation current to reach 63% of the steady state current after commencement of charging.

The trapping parameters N_r, the number of trapping sites per unit volume, and E_b, the binding energy per mol of traps, can be estimated by using the following formula:

$$D_{eff} = D_0 \frac{N_l}{N_r} exp \frac{-(E_b + E_l)}{RT}. \tag{3}$$

N_l is the number of lattice sites per unit volume in the metal, 5.2×10^{32} per cm^3 at ambient temperatures [18].

If D_{eff} is plotted on a logarithmic scale against the inverse of the temperature, the values will ideally fall on a straight line. The expression for this line will be on the form $D_{eff} = Aexp(-B/RT)$. Comparing this expression with equation (3) gives the following relations:

$$N_r = \frac{D_0 N_l}{A} \quad \text{and} \quad E_b = B - E_l, \tag{4}$$

where A and B are the coefficients attained by interpolating the measured values of D_{eff} for various temperatures in the logarithmic plot.

The effective sub-surface hydrogen concentration at the charging surface, C_0, can be obtained by the following formula [19]:

$$C_0 = \frac{J_{ss} L}{D_{eff}} = \frac{i_{ss} L}{F D_{eff}}, \tag{5}$$

where J_{ss} and i_{ss} are the hydrogen flux and measured current density, respectively and F is the Faraday's constant.

3 Experimental

3.1 Materials Selection

The materials tested in this project were the grade X70 pipeline steel in the as delivered and heat treated condition and weld metal of the type HBQ Coreweld provided by ESAB. The chemical composition of the steels are given in Table 1.

Table 1: *Chemical composition of X70 steel and HBQ weld metal.*

Material	**C**	**Mn**	**Si**	**Al**	**P**	**S**
X70 grade steel	0.09	1.71	0.30	0.05	0.0120	0.0010
HBQ weld metal	0.06	1.24	0.41	0.018	0.007	0.010
	Nb	**V**	**Ni**	**Cr**	**Cu**	**Mo**
X70 grade steel	0.05	0.01	0.05	0.07	0.04	0.02
HBQ weld metal	0.003	0.013	0.56	0.032	0.027	0.008
	Ti	**N**	**O**			
X70 grade steel	0.02	0.0050	–			
HBQ weld metal	0.032	0.003	0.046			

3.2 Permeation Apparatus

The electrochemical hydrogen permeation technique was introduced in 1962 by Devanathan and Stachurski [20], and is implemented in the ISO 17081:2004 [17]. The principle of the method is that hydrogen diffuses through a metal specimen separating two electrochemical cells. At the entrance side, the specimen is cathodically polarized, to form adsorbed hydrogen on the surface. The hydrogen diffuses through the specimen to the anodically polarized exit side where hydrogen is oxidized to H^+-ions and electrons. The generated electrons are measured as an electric current.

The permeation apparatus used in this investigation consisted of a two compartment autoclave, filled with 0.1 M NaOH electrolyte and each cell containing a counter- and a reference electrode. Convection was provided by stirring of the electrolyte during the experiments. The compartments were separated by the steel specimen, which constituted the working electrode in both cells. The effective specimen area was a rounded square with an area of 12.25 cm^2.

The equipment was designed by Cormet Testing Systems, Finland (www. cormet.fi), and allowed tests to be carried out at elevated temperatures. A photo of the equipment is given in Figure 1.

A potentiostat was used to charge the specimen with a constant potential of $-1050\ mV_{Ag/AgCl}$ from the cathodic side. The anodic side of the specimen was kept at a constant potential of $+350\ mV_{Ag/AgCl}$ with another potentiostat. After each permeation transient had been recorded, the specimen was discharged by setting the potential to $+300\ mV_{Ag/AgCl}$ on both sides, removing the diffusible hydrogen from the metal. Current and potential in both cells were

constantly logged during the experiments. Experiments were carried out at 25°C, 50°C and 70°C.

1	Load cell	**6**	Dial indicator and limit switches
2	Pressure sensor	**7**	Gear box with worm gear
3	Upper specimen holder	**8**	Heating/cooling bath
4	Autoclave	**9**	Bobbling bottle
5	Lower specimen holder	**10**	Gas inlet pressure reducer

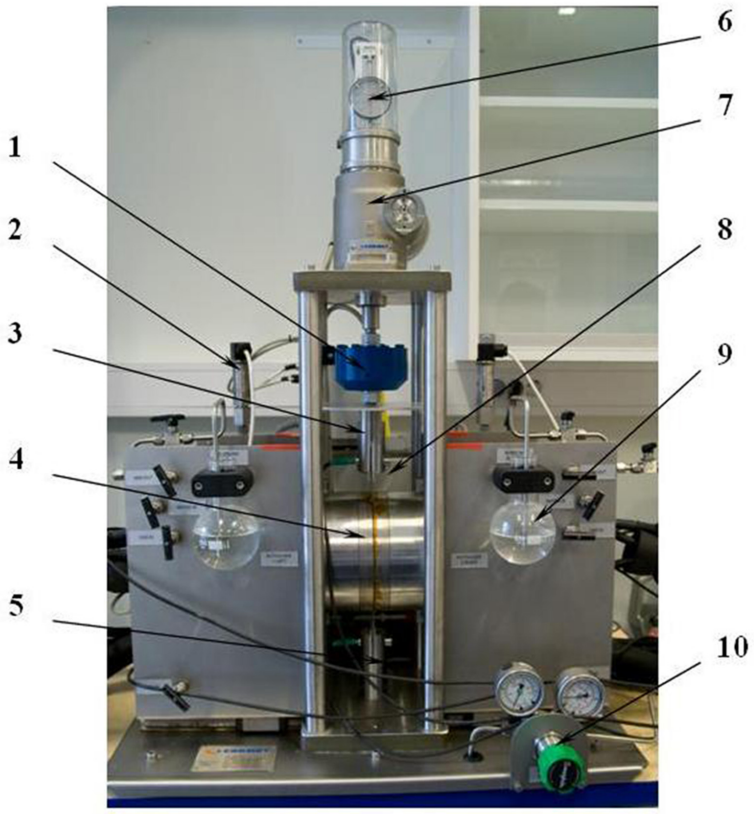

Figure 1: *Design of the permeation apparatus.*

It was not possible to produce a HAZ specimen large enough for the equipment in Figure 1, so a two compartment cell consisting of polycarbonate was used for this microstructure. Temperature regulation was secured by electrolyte circulation through a water bath. It was however only possible to conduct the test at two temperatures, 25°C and 47°C, and only one test was successfully carried out at the elevated temperature. The sample surface of the cell was 7.07 cm^2.

3.3 Specimen Preparation

In order to ensure complete oxidation of hydrogen on the anodic side of the specimen, and to eliminate the risk of oxide formation on the surface, the anodic specimen surface was electrochemically coated with a thin layer of palladium. The procedure for palladium coating followed the recommendations given by P. Manolatos and M. Jerome [21].

The cathodic surface of the specimen was mechanically ground with SiC-paper down to a reproducible 500 grade finish.

Due to severe oxidation of the surface during the heat treatment of the simulated HAZ samples, the sample surfaces had to be machined down to expose the metal. This made it difficult to polish the surface before palladium coating and these samples were therefore used without any further surface preparations after machining.

The specimen thicknesses, and consequently the diffusion lengths, L, were 1.97 mm, 2.06 mm and 1.04 mm for the X70, HBQ and HAZ specimen, respectively (average of ten measurements with an internal deviation less than 5%).

4 Results

4.1 Microstructural Investigations

The microstructure of the different samples was investigated in a light microscope. The base metal X70 grade steel consisted mainly of a fine grained ferritic structure, with darker strands of pearlite with traces of martensite. The weld metal consisted of fine grained acicular ferrite with equiaxial ferrite decorating the prior austenite grain boundaries. The simulated HAZ material consisted of a mixture of bainite and martensite in a structure where the prior austenite grain boundaries were clearly visible.

Microscopical investigations were carried out in both the transverse and the longitudinal direction of the specimens, and the microstructure was found to be isotropic for all three materials.

4.2 Calculation of Diffusion Coefficients and Hydrogen Concentration

4.2.1 X70 Base Metal

Figure 2 shows the permeation transients measured for the X70 steel sample for three different temperatures. Three data sets were recorded for each temperature, and the values vary little for the different tests at the same temperature. One exception is the first transient at 70°C that has a somewhat higher steady state current density than the second and third.

The measured values of i_{ss} and the computed values of D_{eff} and C_0 are given in Table 2.

The effective diffusion coefficient increased by approximately one order of magnitude from the tests carried out at 25°C to the tests carried out at 70°C.

4.2.2 HBQ Weld Metal

Figure 3 shows the permeation transients for the HBQ weld metal measured at three different temperatures. Three transients were recorded at each temperature. Again, the values show some variations in steady state current density, but as it can be seen in Table 3, the values of D_{eff} do not vary accordingly.

4.2.3 Simulated HAZ

Figure 4 shows the permeation transients for the simulated HAZ sample measured in the polycarbonate cell at 25°C and 47°C and the results are given in Table 4. The steady state

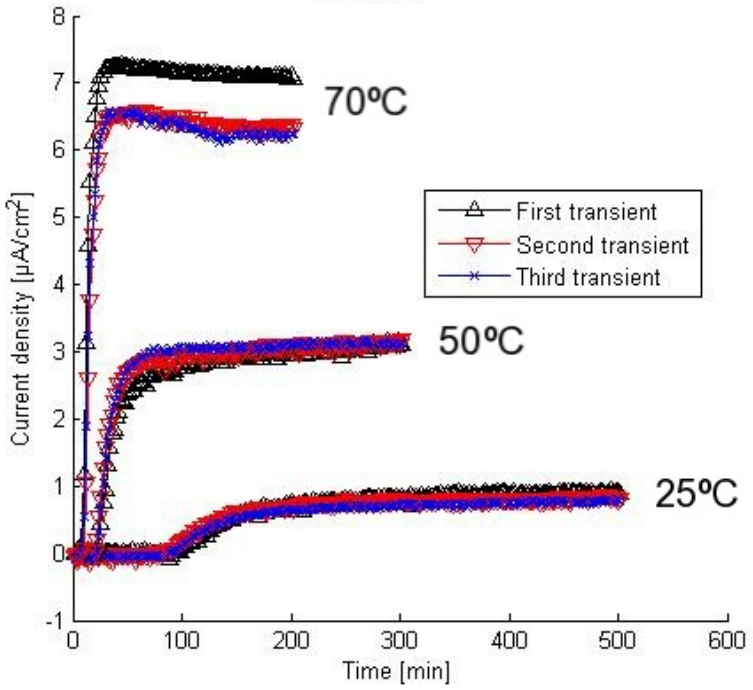

Figure 2: *Permeation current density as function of time, X70 steel.*

Table 2: *Results from permeation experiments on X70 steel.*

Test number	i_{ss} [µA/cm^2]	C_0 [ppm]	D_{eff} [cm^2/s]
25°C, 1	0.872	0.311	7.28×10^{-7}
25°C, 2	0.798	0.261	7.93×10^{-7}
25°C, 3	0.764	0.262	7.59×10^{-7}
50°C, 1	3.12	0.301	2.70×10^{-6}
50°C, 2	3.16	0.274	2.99×10^{-6}
50°C, 3	3.15	0.273	2.99×10^{-6}
70°C, 1	7.24	0.274	7.70×10^{-6}
70°C, 2	6.54	0.268	6.34×10^{-6}
70°C, 3	6.55	0.252	6.74×10^{-6}

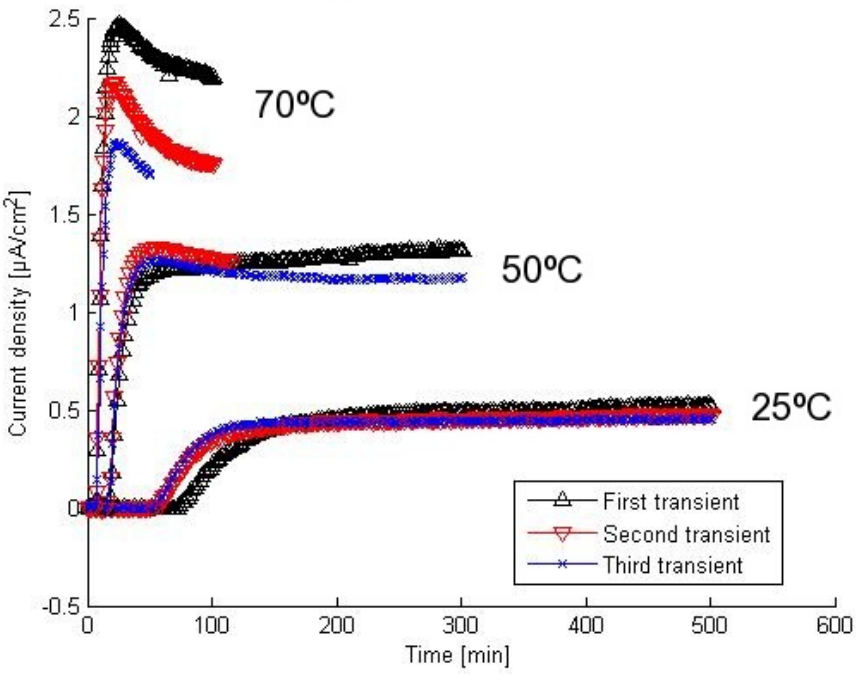

Figure 3: *Permeation current density as function of time, HBQ weld metal.*

Table 3: *Results from permeation experiments on HBQ weld metal.*

Test number	i_{ss} [μA/cm^2]	C_0 [ppm]	D_{eff} [cm^2/s]
25°C, 1	0.494	0.134	9.99×10^{-7}
25°C, 2	0.486	0.105	1.25×10^{-6}
25°C, 3	0.454	0.088	1.40×10^{-6}
50°C, 1	1.20	0.077	4.21×10^{-6}
50°C, 2	1.32	0.079	4.53×10^{-6}
50°C, 3	1.26	0.075	4.53×10^{-6}
70°C, 1	2.46	0.068	9.82×10^{-6}
70°C, 2	2.16	0.055	1.07×10^{-5}
70°C, 3	1.85	0.051	9.82×10^{-6}

current density varied somewhat for the three tests at 25°C, with an increase for each test. The effective diffusion coefficient did not change significantly.

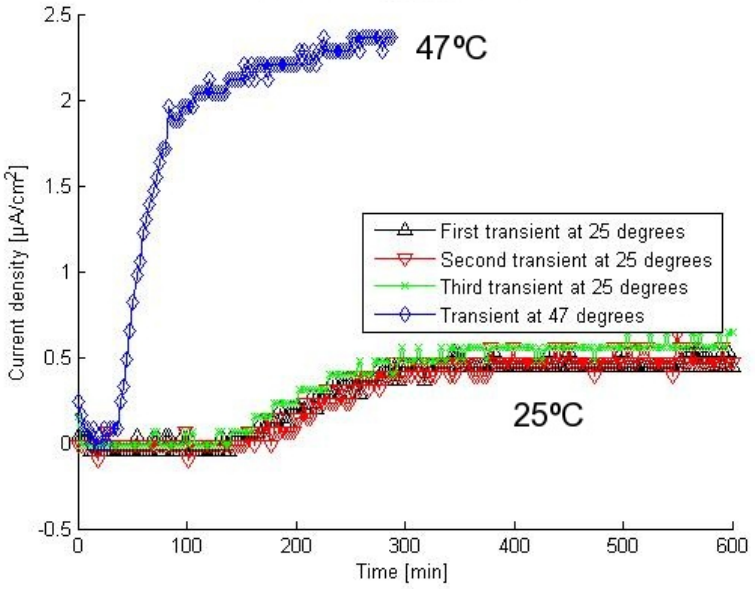

Figure 4: *Permeation current density as function of time, simulated HAZ.*

Table 4: *Results from permeation experiments on simulated HAZ.*

Test number	i_{ss} [µA/cm^2]	C_0 [ppm]	D_{eff} [cm^2/s]
25°C, 1	0.794	0.839	1.30×10^{-7}
25°C, 2	0.846	0.975	1.19×10^{-7}
25°C, 3	0.979	1.04	1.30×10^{-7}
47°C, 1	3.80	1.15	4.53×10^{-7}

4.3 Estimation of Trapping Parameters

Figure 5 gives the measured effective diffusion coefficients as function of inverse temperature for the three materials.

By fitting an exponential function to the data obtained for the effective diffusion coefficient the following relationships between D_{eff} and temperature were found:

$$D_{eff}(X70) = 16exp\left(\frac{-42 \times 10^3}{RT}\right) \tag{6}$$

$$D_{eff}(HBQ) = 14exp\left(\frac{-40 \times 10^3}{RT}\right) \tag{7}$$

$$D_{eff}(HAZ) = 16exp\left(\frac{-46 \times 10^3}{RT}\right) \tag{8}$$

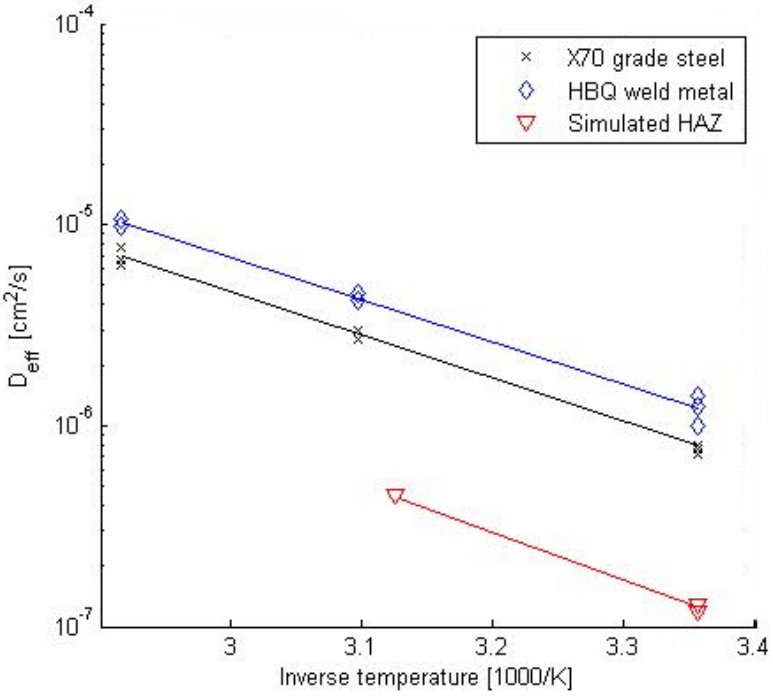

Figure 5: *Effect of temperature on* D_{eff}.

By comparing equation (6) with equation (3) the trapping parameters can be estimated for the X70 base metal:

$$N_r = \frac{D_0 N_l}{16} = \frac{7.23 \times 10^{-4} \times 5.2 \times 10^{23}}{16}$$

$$= 2.3 \times 10^{19}\ sites/\mathrm{cm}^3,$$

$$E_b = 42 \times 10^3 - E_l = (42 - 5.69) \times 10^3$$

$$= 36\ \mathrm{kJ/mol}.$$

The same procedure was carried out for the two other metals and the results are given in Table 5.

5 Discussion

5.1 Microstructure – Diffusion Coefficient Relations

The effective diffusion coefficients measured in the different materials do not differ greatly, but some consistent variations could be seen between the values obtained. There is a large scatter

Table 5: *Estimated values of N_r and E_b for the three different metals.*

Material	Formula	N_r [$sites/\mathrm{cm}^3$]	E_b [kJ/mol]
X70 grade steel	$D_{eff} = 16exp\left(\frac{-42\times10^3}{RT}\right)$	2.3×10^{19}	36 ± 1
HBQ weld metal	$D_{eff} = 14exp\left(\frac{-40\times10^3}{RT}\right)$	2.7×10^{19}	34 ± 1
Simulated HAZ	$D_{eff} = 16exp\left(\frac{-46\times10^3}{RT}\right)$	2.3×10^{19}	41 ± 3

in the reported effective diffusion coefficients for ferritic steel, ranging between 5×10^{-9} to 10^{-6} cm^2/s [22] at room temperature, making it difficult to compare the obtained result with any accuracy to existing results. Park et al. [14] have however estimated values of D_{eff} for a steel of grade X65 ranging between 4.05 and 9.38×10^{-6} cm^2/s at room temperature. These values are somewhat higher than the values obtained for X70 in this project, with measured values between 7.28 and 7.93×10^{-7} cm^2/s. This may be due to the slightly higher alloying level in X70, since increased alloying tends to slow down diffusion.

Compared with the X70 grade steel, the HBQ weld metal showed higher effective diffusion coefficients for all temperatures. The diffusion coefficient in HBQ weld metal showed a response to temperature similar to that of the X70 grade metal.

The simulated HAZ gave the lowest values for the effective diffusion coefficient, with a D_{eff} of approximately 1×10^{-7} cm^2/s at room temperature. Although a limited amount of data was available at the higher temperature, the estmated D_{eff} at 47°C indicated a temperature response similar to the two other metals.

In the values of D_{eff} for the HBQ weld metal and the X70 grade steel at 25°C, an increase can be seen from the first to the second permeation. This may be a result of irreversible traps being filled during the first transient. The filled irreversible traps will not affect the hydrogen permeation during the consequent transients, and the measured effective diffusion coefficient will be higher. The effect was most profound for the HBQ weld metal with a 25% increase for the second transient. For the X70 grade steel, the increase was only 8% and for the simulated HAZ, there was no increase in D_{eff}.

5.2 Effect of Microstructure on C_0, N_r and E_b

The measured value of C_0 for the three materials did not vary significantly with temperature, as the higher steady state current was balanced by a higher diffusion coefficient. The average sub-surface hydrogen concentrations were 0.27 ppm, 0.081 ppm and 1.00 ppm for the X70, HBQ and HAZ specimen, respectively.

A source of error in the measurement of C_0 for the simulated HAZ sample is the fact that proper grinding of the sample surface was not possible. This may have lead to an incomplete palladium layer on the anodic surface, again leading to recombination of hydrogen atoms, rather than oxidation, on the anodic side of the specimen.

The estimation of number of traps per unit volume gave similar values for all three microstructures investigated, around 2.5×10^{19} traps per cubic centimeter. Estimation of binding energy of these traps gave a slightly higher value for the HAZ specimen, i.e. 41 kJ/mol, than for the X70 and HBQ specimen with values of 36 and 34 kJ/mol, respectively. This pattern follows that of D_{eff} for the three alloys at 25°C with a higher binding energy corresponding to

a low diffusion coefficient.

As the parameter estimations for the HAZ sample is only based on one measurement at an elevated temperature, a definite conclusion can not be drawn on this material. The temperature effect on D_{eff} measured for HAZ did, however, greatly resemble those of the X70 and the HBQ samples.

6 Conclusion

- The average effective diffusion coefficient at room temperature varied for the different materials as 7.60×10^{-7} cm^2/s for the X70 grade steel, 1.22×10^{-6} cm^2/s for the HBQ weld metal and 1.26×10^{-7} cm^2/s for the simulated HAZ. The effective diffusion coefficients for the different materials showed similar response to increased temperature, and an expression on the Arrhenius form was estimated for all three.

- The sub-surface hydrogen concentration was found to be quite similar for the three materials, between 0.1 and 1 ppm at 25°C. The temperature influence on the value was limited, as the increased flux was balanced by a higher diffusion coefficient.

- The number of reversible traps was found to be approximately 2.5×10^{19} sites/cm^3 for all three materials. Evidence of irreversible trapping was seen for the X70 steel and the HBQ weld metal.

- The average binding energy of the reversible traps in the different materials was estimated. The values varied between 34 and 41 kJ/mol for the HBQ weld metal and simulated HAZ, respectively, with the value for the X70 grade steel being 36 kJ/mol.

7 Acknowledgements

The present work was financed by the Research Council of Norway (Petromaks project 192967/S60), Statoil, Technip and EFD Induction. The authors wish to thank Mr Hans Fostervoll, SINTEF, for providing the weldments for testing.

References

[1] H. K. Birnbaum and P. Sofronis. Hydrogen-enhanced localized plasticity – a mechanism for hydrogen-related fracture. *Material Science and Engineering*, A176:191–202, 1994.

[2] P. J. Ferreira, I. M. Robertson, and H. K. Birnbaum. Hydrogen effects on the interaction between dislocations. *Acta Materialia*, 46(5):1749–1757, 1998.

[3] W. W. Gerberich, P. G. Marsh, and J. W. Hoehn. Hydrogen induced cracking mechanisms – are there critical experiments? *Hydrogen Effects in Materials*, pages 539–551, 1996.

[4] Jr C. J. McMahon, X. Liu, J. Kameda, and M. J. Morgan. Recent Observation of Hydrogen-Induced Cracking of High-Strength Steels. *Proceedings of the 2008 International Hydrogen Conference*, pages 46–53, 2008.

[5] P. Nevasmaa. Hydrogen cold cracking in high-strength multipass weld metal – a procedure for predicting the cracking risk and necessary precautions for safe welding. In *Document IX-2088-04*, pages 1–26. 57th annual assembly of the international institute of welding (IIW), Osaka, Japan, 11-16 july 2004.

[6] A. Taha and P. Sofronis. A micromechanics approach to the study of hydrogen transport and embrittlement. *Engineering Fracture Mechanics*, 68:803–837, 2001.

[7] P. Zimmer, T. Boellinghaus, and T. Kannengiesser. Effects of hydrogen on weld microstructure mechanical properties of the high strength steels S 690Q and S 1100QL. *IIW Doc. II-A-141-04*, pages 1–20, 2004.

[8] I. M. Robertson, D. Lilling, and D. J. Ferreira. Revealing the fundamental processes congrolling hydrogen embrittlement. *Proceedings of the 2008 International Hydrogen Conference*, pages 22–37, 2008.

[9] W. W. Gerberich, D. D. Stauffer, and P. Sofronis. A Coexistent View of Hydrogen Effects on Mechanical Behaiour of Crystals: HELP and HEDE. *Proceedings of the 2008 International Hydrogen Conference*, pages 38–45, 2008.

[10] A. R. Troiano. The role of hydrogen and other interstitials in the mechanical behavior of metals. In *1959 Edward De Mille Campbell Memoral Lecture*, pages 54–80. 41st Annual Convension of the American Society for Metals, 1959.

[11] W. W. Gerberich, R. A. Oriani, M.-J. Lii, X Chen, and T. Foecke. The necessity of both plasticity and brittlenes in the fracture thresholds of iron. *Philosophical Magazine A*, 63(2):363–376, 1990.

[12] Ø. Grong. *Metallurgical Modelling of Welding*, chapter 7. The Institute of Materials, 2nd edition, 1997.

[13] P. Nevasmaa and A. Laukkanen. Procedure for the prevention of hydrogen cracking in multipass weld metal with emphasis on the assessment of cracking risk in 2.25cr-1mo-0.25v-tib (T24) boiler steel. In *Document IX-2131-04*, pages 1–38. 57th annual assembly of the international institute of welding (IIW), Osaka, Japan, 11-16 july 2004.

[14] G. T. Park, S. U. Koh, H. G. Jung, and K. Y. Kim. Effect of microstructure on the hydrogen trapping efficiency and hydrogen induced cracking of linepipe steel. *Corrosion science*, 50:1865–1871, 2008.

[15] S. H. Wang, W. C. Luu, K. F. Ho, and J. K. Wu. Hydrogen permeation in a submerged arc weldment of tmcp steel. *Materials Chemistry and Physics*, 77:447 – 454, 2002.

[16] K. Kiuchi and R. B. McLellan. The solubility and diffusivity of hydrogen in well-annealed and deformed iron. *Acta Metallurgica*, 31(7):961–984, 1983.

[17] International Standard Organization. *ISO 17081:2004, Method of measurement of hydrogen permeation and determination of hydrogen uptake and transport in metals by an electrochemical technique*, 2004.

[18] A. Turnbull, M.W. Carroll, and D. H. Ferriss. Analysis of hydrogen diffusion and trapping in a 13 % chromium martensitic stainless steel. *Acta Metallurgica*, 37(7):2039–2046, 1989.

[19] R. A. Oriani. The diffusion and trapping of hydrogen in steel. *Acta Metallurgica*, 18:147–157, 1970.

[20] M. A. V. Devanathan and Z. Stachurski. The absorption and diffusion of hydrogen in palladium. *Proceedings of the Royal Society of London. Series A, Mathematical and Physical Sciences*, 270(1340):90–102, October 1962.

[21] P. Manolatos and M. Jerome. A thin palladium coating on iron for hydrogen permeation studies. *Electrochimica Acta*, 41(3):359–365, 1996.

[22] K. Easterling. *Introduction to the Physical Metallurgy of Welding*, chapter 4. Buttersworth-Heinemann Ltd, 2^{nd} edition, 1992.